Journal of Human Evolution 60 (2011) 106–116

Contents lists available at ScienceDirect

Journal of Human Evolution

journal homepage: www.elsevier.com/locate/jhevol

Relationships between the expression of the stapedial artery and the size of the obturator foramen in euarchontans: Functional and phylogenetic implications

Mark N. Coleman [a,*], Doug M. Boyer [b]

[a] Department of Anatomy, Midwestern University, 19555 N. 59th Ave., Glendale, AZ 85308, United States
[b] Department of Anthropology and Archaeology, Brooklyn College, CUNY, 2900 Bedford Ave., Brooklyn, NY 11210, United States

ARTICLE INFO

Article history:
Received 5 November 2008
Accepted 30 September 2010

Keywords:
Plesiadapiform
Scandentia
Dermoptera
Primates
Systematics
Cranial blood supply
Stapes
Stapedial canal

ABSTRACT

Cranial arterial patterns are commonly used for determining phylogenetic patterns in extant taxa and have often been used in studies investigating the relationships among fossil taxa. In primitive eutherians, the stapedial artery provided blood to the meninges, orbits, and certain regions of the face. In many modern mammals, however, blood supply to most of these areas has been taken over by branches of the external carotid, although some groups (e.g., treeshrews, some families of primates) still retain aspects of the ancestral pattern. Here, we show that the relative size of the obturator foramen of the stapes is a reliable indicator of the presence or absence of a "functional" stapedial artery in Euarchonta. We also describe newly discovered stapedes for extinct euarchontans, *Ignacius graybullianus*, and *Plesiadapis tricuspidens*, and use the approach described here to show that these taxa likely did not have a functional stapedial artery. The implications of these findings for auditory function and phylogenetic studies are discussed.

Introduction

Cranial circulation patterns in mammals have proven to be informative for inferring phylogenetic relationships at various taxonomic levels (Szalay and Katz, 1973; Bugge, 1974; Wahlert, 1974; Cartmill, 1975; Saban, 1975; Szalay, 1975; Cartmill and MacPhee, 1980; MacPhee, 1981; MacPhee and Cartmill, 1986; Wible, 1986, 1987; Schwartz and Tattersall, 1987; Wible, 1993; Wible and Zeller, 1994). The primitive eutherian arterial pattern (Fig. 1A) has been reconstructed to show that the internal carotid artery was one of two major vessels providing blood to the brain (in addition to the vertebral a.), while many major regions of the skull (excepting the tongue and pharynx) were supplied by its first major branch, the stapedial artery (Bugge, 1974; Wible, 1987). After passing through the intercrural (obturator) foramen of the stapes, the stapedial artery divided into a superior ramus, which supplied the extrabullar structures of the orbit and the meninges, and an inferior ramus, which supplied structures in the infraorbital and mandibular (inferior alveolar) regions. Modern orders retain various aspects of this pattern although in most groups, branches of the external carotid take over the blood supply to many of the regions supplied by the stapedial artery, and its branches become reduced or entirely absent (i.e., involuted). Primitive euprimates also possessed a well-developed stapedial artery with numerous branches (Diamond, 1991), although living primates have evolved several variations on the ancestral primate (and eutherian) pattern.

Among extant primates, certain families of strepsirhines (Fig. 1B) show similarities to the presumed ancestral condition by possessing a well-developed stapedial artery, although no known species has been shown to retain a "functional" inferior ramus branch of the stapedial in the adult stage (MacPhee and Cartmill, 1986). Three families of lemuroids (Lemuridae, Indriidae, and Daubentoniidae) are characterized by having a large stapedial artery supplying the meninges and orbital tissues in association with a relatively small distal internal carotid (Saban, 1975; MacPhee and Cartmill, 1986). However, species of the family Cheirogaleidae (Fig. 1C) have a greatly reduced internal carotid system, counterbalanced by a well-developed ascending pharyngeal artery that helps supply blood to the brain and orbits, similar to the pattern found in lorisiforms (Cartmill, 1975; Butler, 1980). Members of Lepilemuridae (Fig. 1D) demonstrate yet another pattern by having reduced internal carotid, vestigial stapedial, and non-hypertrophied ascending pharyngeal arteries (Schwartz and Tattersall, 1987), apparently relying almost exclusively on the vertebral and external carotid arteries for cranial blood supply (Szalay and Katz, 1973; MacPhee, 1987).

Anthropoids are noted to possess a large internal carotid artery and partial or complete obliteration of the stapedial artery (Bugge,

* Corresponding author. Tel.: +1 623 572 3714; fax: +1 623 572 3679.
E-mail addresses: mcolem@midwestern.edu (M.N. Coleman), douglasmb@gmail.com (D.M. Boyer).

0047-2484/$ – see front matter © 2010 Elsevier Ltd. All rights reserved.
doi:10.1016/j.jhevol.2010.09.006

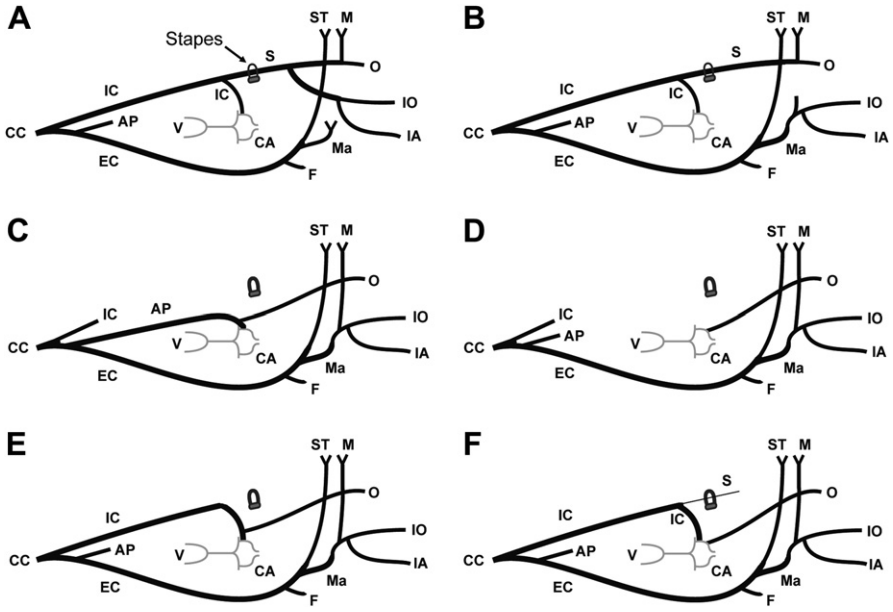

Figure 1. Cranial circulation patterns in extant primates. A. Hypothetical reconstruction of the primitive eutherian pattern (based on Wible, 1987). A similar pattern is retained in living treeshrews (Wible and Zeller, 1994). B. Lemuridae, Indriidae, and Daubentoniidae (based on Saban, 1975 and MacPhee and Cartmill, 1986). C. Cheirogaleidae and lorisoids (based on Cartmill, 1975). D. Lepilemuridae (based on Szalay and Katz, 1973 and MacPhee, 1987). A somewhat similar pattern is seen in extant Dermoptera with the reduction of the internal carotids, although colugos also receive blood to the orbits from the maxillary artery (Wible, 1993). E. Anthropoids (based on Bugge, 1974). F. Tarsiers (based on Hill, 1953; Saban, 1963; and MacPhee and Cartmill, 1986). Abbreviations: AP = ascending pharyngeal; CA = circulus arteriosus; CC = common carotid; EC = external carotid; F = facial; IA = inferior alveolar; IC = internal carotid; IO = infraorbital; M = meningeal; Ma = maxillary; O = orbital/ophthalmic; S = stapedial; ST = superficial temporal; V = vertebral.

1974). In adult monkeys and apes (Fig. 1E), the ophthalmic artery (arising from the distal internal carotid a.) supplies the orbital region, while the meninges get most of their blood from the maxillary artery (a branch of the external carotid a.). Tarsiers (Fig. 1F) also manifest a large internal carotid artery but the degree of development of the stapedial artery remains poorly resolved. Although tarsiers have a bony canal that passes through the obturator foramen, there are conflicting reports as to whether or not this canal transmits an artery (stapedial) with a patent lumen (e.g., Hill, 1953; Saban, 1963). Regardless, the areas normally supplied by the superior ramus of the stapedial artery are annexed by other vessels, somewhat similar to the pattern witnessed in anthropoids. The meninges are supplied by the external carotid, although the exact branch has been identified as either the maxillary (Hill, 1953; Saban, 1963), the posterior auricular (Hafferl, 1916), or possibly both (MacPhee and Cartmill, 1986). In addition, orbital tissues receive blood from the ophthalmic artery, which arises from the circulus arteriosus (Hill, 1953). Consequently, as a result of the diminished nature of the stapedial artery and the fact that most of its regions of supply are taken over by other branches of the internal and external carotids, most researchers consider the stapedial artery in tarsiers to be either vestigial (Schwartz and Tattersall, 1987) or non-functional (Kay et al., 1997).

Because these arteries generally leave various bony markers of their presence, arterial patterns can often be reconstructed in fossils and have figured prominently in debates about the relationships of extinct taxa to modern groups (Gingerich, 1973, 1976; Archibald, 1977; Wible, 1983; MacPhee, 1987; Kay et al., 1992; Silcox, 2003). However, many of the bony canals, grooves, and foramina that transmit these vessels also convey other neurovascular structures, which can make it difficult to determine whether or not an artery was functionally present with a patent lumen that transmitted blood in the adult (Kanagasuntheram and Krishnamurti, 1965; Bugge, 1974; Cartmill, 1975; Conroy and Wible, 1978). Even in cases where a canal is not known to be associated with any nervous structures (e.g., stapedial canal), the simple presence of a canal (particularly ones that are relatively small) does not necessarily indicate a functional artery in the adult stage (as seems to be the case with tarsiers – see below). Furthermore, some taxa, such as certain species of microchiropteran bats, have a well-developed basicranial arterial pattern that does not leave distinctive bony markers of its presence (Wible and Davis, 2000).

Why these patterns are particularly informative is not known. However, it may be that their complexity and their insulation from external environmental selection pressures reduces the frequency of convergent cranial blood supply patterns, as compared to anatomy involved in feeding or locomotion such as teeth, most postcranial bones, or both teeth and postcrania. One can imagine demands on sensory systems that would select for one pattern over the other; in that case, another reason for conservation of this system could be that because of its role in keeping the brain and sense organs functioning, a more typical level of variation might yield lethality, instead of increased diversity to be targeted by natural selection.

In this study, we investigate the relationship between the size of the obturator foramen of the stapes and the degree of development of the stapedial artery in a broad sample of extant primates as well as other extant members of orders placed in the cohort Euarchonta, including dermopterans and scandentians. We test the hypothesis that the obturator foramen functions primarily to transmit the stapedial artery. If this hypothesis holds, then the obturator foramen should be relatively larger in taxa with a functional, relatively large artery than in taxa with a non-functional, relatively small or absent artery. We then use the data from extant species to explore the condition of the stapedial artery in two extinct species of plesiadapiform euarchontans.

Materials and methods

The morphology of the stapes associated with a functional or non-functional stapedial artery was assessed by comparing the

area of the obturator foramen with the overall size of the stapes. The length of the long axis of the stapedial footplate was taken as a proxy for the overall size of the stapes. A species was considered to have a "functional" stapedial artery if that species has been documented to have a stapedial artery with on open lumen and retains at least one of its major branches (e.g., superior ramus). Our extant comparative sample consisted of 41 species of primates (122 specimens) including individuals representing all major cranial blood supply patterns found in living primates. We also examined four species of non-primate euarchontans for outgroup comparisons: *Tupaia glis* ($n = 1$), *Ptilocercus lowii* ($n = 4$), *Cynocephalus volans* ($n = 1$), and *Galeopterus variegatus* ($n = 1$). Both species of treeshrews (*T. glis* and *P. lowii*) have been shown to have a functional stapedial artery that maintains many of the branches of the hypothetical ancestral pattern (Bugge, 1974; Wible and Zeller, 1994), while adult colugos essentially lack stapedial and internal carotid arteries altogether (Wible, 1993).

The majority of specimens examined were isolated stapedes that were associated with dry skulls from the collections at the American Museum of Natural History, Field Museum of Natural History, National Museum of Natural History, and Stony Brook Anatomical Museum. A few stapedes were extracted from cadavers that retained soft tissue. In these cases, we attempted to observe (and if possible document) the arterial pattern in order to check the accuracy of published descriptions of circulation patterns. For instance, we observed that *Eulemur fulvus* (SBAM-Efr 3562f – originally purchased from Duke Lemur Center by S. Larson) had patent internal carotid arteries (proximal and distal to the stapedial a.) and a right stapedial artery that was patent and roughly the same diameter as the distal internal carotid artery on the same side. However, the stapedial artery could not be located on the left side, possibly indicating that it was not developed or functional in life. Although this observation does not refute the generalization that all species of Lemuridae have a well-developed stapedial artery, it definitely demonstrates the need for more detailed studies of arterial dominance within families and between individuals.

For specimens with isolated stapedes, measurements were made by first taking digital photographs of stapedes under low magnification from multiple angles, along with a scale, at a distance that minimized problems associated with parallax (Spencer and Spencer, 1995). Next, the digital images were imported into SigmaScan Pro 5.0 image measurement software, calibrated, and measured using the trace mode function. The surface area of the obturator foramen was estimated by outlining the inner circumference of the crura and footplate. Because the stapedial crura of the specimens examined here are not tubular structures, but instead display more of a U-shaped morphology in cross section, there are actually two obturator foramina for each stapes. This is illustrated in Fig. 2, where it can be seen that the foramen on the ventral side (white arrows) is considerably smaller that the foramen on the dorsal side (black arrows). Therefore, stapedes were imaged and measured on both sides and the side with the smaller surface area was taken as the final value, because it is assumed that the smaller foramen will have the closest association with the stapedial artery.

The fossil specimens investigated here are two previously undescribed stapedes that were discovered within the vestibule of the inner ear during CT scanning. We suspect that there may be additional fossil stapedes in museum collections that have been preserved by falling into the inner ear during fossilization. The first stapes comes from a fragmentary skull of *Ignacius graybullianus* (USNM 482353) housed in the Smithsonian collections at the National Museum of Natural History. This taxon lived in North America during the early Eocene and likely had a body mass between 231 g (based on cranial length) and 375 g (based on dental measurements) (Silcox et al., 2009a). The second stapes was found

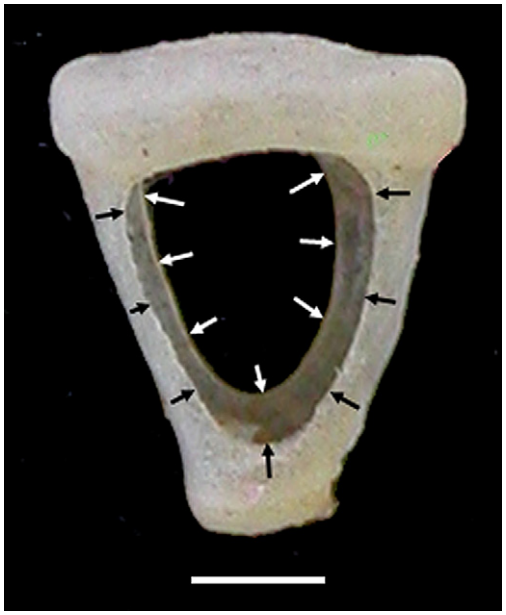

Figure 2. Image of *Cebus capucinus* stapes illustrating the difference in obturator foramen areas between the ventral and dorsal surfaces. In this specimen, the ventral obturator foramen (white arrows) has an estimated area of 55 mm^2 compared to a value of 84 mm^2 for the dorsal obturator foramen (black arrows). All specimens were imaged and measured on both sides and the side with the smaller surface area was taken as the final value. Scale bar = 0.5 mm.

in an isolated petrosal bone of *Plesiadapis tricuspidens* (MNHN BR 17418) from the collections at the Museum Nationale d'Histoire Naturelle, Paris. This was a medium sized animal (~2656 g, based on dental measurements [Silcox et al., 2009b]) that was unearthed in late Paleocene deposits of the Berru locality near Cernay-lès-Reims, France. Both species are members of extinct clades of plesiadapiforms, which have been placed as stem primates in comprehensive phylogenetic analyses (Bloch et al., 2007).

The fossil ossicles were "virtually extracted" using high resolution X-ray computed tomography (CT) data. The stapedes were isolated by manually segmenting the ear bones from the surrounding structures in each CT slice. Using these segmented slices, three dimensional models of the stapedes (*in situ*) were created using 3D Slicer 2.6 open source software, and measurements were taken on 2D digital images of the 3D models using the same method described above for the extant material. Threshold values used to construct the digital models were based upon the half-maximum height protocol described in Coleman and Colbert (2007), using the stapedial crura as the region of interest. USNM 482353 was imaged in the Department of Biomedical Engineering Center for Biotechnology at Stony Brook University, producing cubic voxels of 6 microns. MNHN BR 17418 was scanned at the Center for Quantitative Imaging, Pennsylvania State University, and had voxel dimensions of 50 × 50 × 58 microns. In addition, intact stapedes for four extant species were digitally extracted and measured using the same method as applied to the fossils: *Tarsius spectrum*, *Ptilocercus lowii*, *Cynocephalus volans*, and *Galeopterus variegatus*. The tarsier specimens (10 × 10 × 10 microns) were scanned at Stony Brook University, the treeshrews (24 × 24 × 26 microns) were scanned at the high resolution X-ray CT facility at the University of Texas at Austin, and the colugos (41 × 41 × 50 microns) were scanned at the Center for Quantitative Imaging, Pennsylvania State University.

The species mean values of stapedial measurements for all specimens are given in Table 1. All measurements used in the

Table 1
Species mean values for stapedial footplate length, obturator foramen area, body mass, and area ratio (square root of obturator area/stapedial footplate length) for all taxa investigated in this study. Extant primate body mass data taken from Smith and Jungers (1997), body mass for treeshrews from Askay (2000), and body mass for colugos from Myers (2000). Numbers in parentheses represent the number of specimens assayed for each species. See text for discussion of arterial patterns.

Species	Arterial pattern	Footplate length (mm)	Foramen area (mm^2)	Body mass (g)	Area ratio
Alouatta caraya (6)	Non-stapedial	1.72	0.58	5375	0.44
Alouatta seniculus (2)	Non-stapedial	2.03	0.72	6087	0.42
Aotus azarae (8)	Non-stapedial	1.36	0.35	1200	0.44
Aotus nancymae (3)	Non-stapedial	1.40	0.33	787	0.41
Aotus trivirgatus (3)	Non-stapedial	1.30	0.26	775	0.39
Aotus vociferans (1)	Non-stapedial	1.37	0.40	703	0.46
Arctocebus calabarensis (2)	Non-stapedial	1.23	0.32	309	0.46
Ateles paniscus (6)	Non-stapedial	2.06	0.93	8775	0.47
Cacajao calvus (1)	Non-stapedial	1.35	0.35	3165	0.44
Cacajao melanocephalus (1)	Non-stapedial	1.39	0.24	2935	0.35
Callicebus sp. (3)	Non-stapedial	1.29	0.30	1005	0.43
Callithrix jacchus (6)	Non-stapedial	1.13	0.08	321	0.25
Cebuella pygmaea (1)	Non-stapedial	1.10	0.16	116	0.37
Cebus albifrons (3)	Non-stapedial	1.54	0.01	2735	0.06
Cebus apella (10)	Non-stapedial	1.59	0.31	3085	0.35
Cercopithecus mitis (1)	Non-stapedial	1.80	0.55	6030	0.41
Cercopithecus neglectus (3)	Non-stapedial	1.92	0.74	5740	0.45
Chiropotes satanas (4)	Non-stapedial	1.39	0.18	2885	0.31
Chlorocebus aethiops (2)	Non-stapedial	1.78	0.69	4240	0.47
Cynocephalus volans (1)	Non-stapedial	1.62	0.32	1350	0.35
Daubentonia madagascariensis (1)	Stapedial	1.88	0.96	2560	0.52
Erythrocebus patas (2)	Non-stapedial	1.99	0.76	9450	0.44
Eulemur fulvus (1)	Stapedial	1.62	0.84	2215	0.57
Galeopterus variegatus (1)	Non-stapedial	1.47	0.33	1100	0.39
Galago senegalensis (6)	Non-stapedial	1.18	0.21	248	0.39
Indri indri (1)	Stapedial	1.69	0.88	6335	0.55
Lagothrix lagotricha (3)	Non-stapedial	1.99	0.57	7683	0.38
Lemur catta (1)	Stapedial	1.47	0.64	2210	0.54
Leontopithecus rosalia (1)	Non-stapedial	1.42	0.20	609	0.32
Lepilemur mustelinus (2)	Non-stapedial	1.42	0.34	777	0.41
Loris tardigradus (2)	Non-stapedial	1.16	0.30	230	0.48
Macaca fascicularis (4)	Non-stapedial	1.76	0.58	4475	0.43
Nycticebus coucang (2)	Non-stapedial	1.09	0.23	653	0.44
Pithecia monachus (2)	Non-stapedial	1.60	0.30	2360	0.34
Pithecia pithecia (1)	Non-stapedial	1.55	0.35	1760	0.38
Perodicticus potto (11)	Non-stapedial	1.23	0.27	1032	0.42
Phaner furcifer (1)	Non-stapedial	1.34	0.49	460	0.52
Propithecus diadema (2)	Stapedial	1.60	0.63	6100	0.50
Ptilocercus lowii (1)	Stapedial	0.83	0.28	51	0.64
Saguinus sp. (1)	Non-stapedial	1.17	0.30	411	0.46
Saimiri boliviensis (7)	Non-stapedial	1.12	0.20	811	0.40
Saimiri sciureus (1)	Non-stapedial	1.12	0.19	790	0.39
Tarsius spectrum (3)	Non-stapedial	0.90	0.17	116	0.46
Tupaia glis (1)	Stapedial	0.98	0.48	180	0.71
Varecia variegata (1)	Stapedial	1.53	0.95	3533	0.64
Ignacius graybullianus (USNM 482353)	Non-stapedial?	1.08	0.20	231–375	0.41
Plesiadapis tricuspidens (MNHN BR 17418)	Non-stapedial?	1.49	0.33	2656	0.39

analyses were found to be normally distributed using a Kolmogorov–Smirnov test (footplate length, $p = 0.812$; square root of obturator foramen area, $p = 0.188$; cube root of body mass, $p = 0.463$). In addition to using conventional statistical techniques (computed using SPSS 16.0 analytical software), these data were also analyzed using phylogenetic comparative methods via the PDAP package (Midford et al., 2010) in Mesquite 2.73, a modular system for evolutionary analysis (Maddison and Maddison, 2010). The phylogenetic tree used in these analyses is shown in Fig. 3.

Results

Extant comparative sample

To investigate the relationship between the size of the stapes and overall body size, stapedial footplate length was regressed against the natural log of the cube root of body mass for all taxa investigated (Fig. 4A). Considering all of the taxa together, there is a significant relationship between stapedial footplate length and body mass, whether using conventional regression analysis ($p < 0.001$, $r^2 = 0.797$) or phylogenetically informed analysis ($p < 0.001$, $r^2 = 0.526$). Both analyses reveal that the footplate scales with negative allometry, similar to other middle and inner ear structures (Cartmill, 1975; Fleischer, 1978). These results show that species with a functional stapedial artery are intermixed among the taxa with a non-functional artery. In fact, the difference between groups in the relative length of the footplate (footplate length/cube root of body mass) is non-significant using a Mann–Whitney U test ($p = 0.570$). This finding suggests that having a functional stapedial artery does not influence footplate length, and that footplate length is a valid proxy for overall size. Also plotted in this graph are the values for the fossil stapedes; both specimens fall just below the best-fit line (regardless of technique), indicating that there is nothing unusual about the footplate length in these specimens given body masses estimated by Silcox et al. (2009a,b).

Next, the square root of obturator foramen area was plotted against stapedial footplate length (Fig. 4B). These analyses appear to reveal a separation of taxa with a functional stapedial artery from

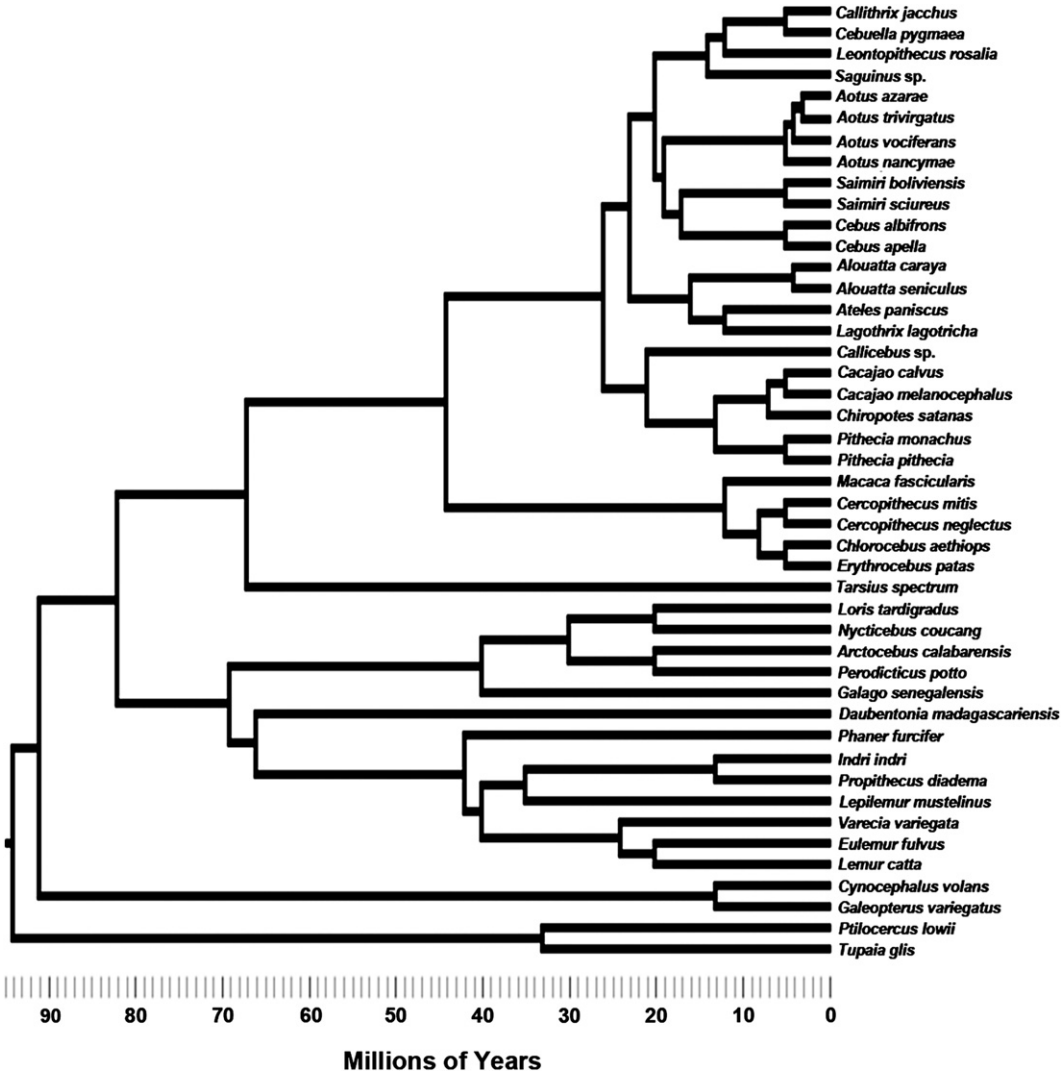

Figure 3. Phylogenetic tree used in this analysis. The relationships and time of origin for Primates, Dermoptera, and Scandentia, as well as the time of basal diversification for treeshrews and colugos, are based on Bininda-Emonds et al. (2007). The LCA for primates (haplorhine–strepsirhine split) is based on Tavaré et al. (2002). The diversification of lemuroids from lorisoids and of galagids from lorisids is based on Yoder and Yang (2004). The divergence of *Nycticebus* from *Loris*, *Daubentonia* from other lemuroids, as well as the splits within members of the lemuridae, are based on Horvath et al. (2008). The other branching points within lemuroids are based on arguments presented in Coleman and Ross (2004). The split between *Perodicticus* and *Arctocebus* was arbitrarily set at 20 Ma (similar to that for *Nycticebus* from *Loris*) and the divergence of this group from the other lorises was set at 30 Ma (midpoint). The branching of tarsiers from anthropoids and between catarrhines and platyrrhines is based on Hodgson et al. (2009). The relationships and divergence times for all catarrhines are based on Tosi et al. (2005). The genus level relationships and divergence times for platyrrhines are based on Opazo et al. (2006). The internal relationships and branching times for *Aotus* are based on Menezes et al. (2010) and those for *Alouatta* are based on Cortés-Ortiz et al. (2003). All other internal (species) branching times for New World monkeys (e.g., *Cebus apella* vs. *Cebus albifrons*) were arbitrarily set at 5 Ma (similar to the known diversification times for *Aotus* and *Alouatta*).

those with a non-functional artery. Using conventional regression analysis, obturator foramen area is not as highly correlated with stapedial foot length ($p < 0.001$, $r^2 = 0.465$), as the latter dimension is to body mass. However, the relationship between obturator foramen area and stapedial length is stronger if taxa with a non-functional stapedial artery are considered separate from those with a functional artery (non-functional artery regression: $p < 0.001$, $r^2 = 0.574$; functional artery regression: $p = 0.002$, $r^2 = 0.825$). A similar pattern was detected using phylogenetic comparative methods (non-functional artery regression: $p = 0.003$, $r^2 = 0.222$; functional artery regression: $p = 0.031$, $r^2 = 0.556$). It appears that, for a given stapedial footplate length, those taxa with a functional stapedial artery have a larger obturator foramen. Comparing the relative size of the obturator foramen (square root of obturator foramen area/stapedial footplate length), there is a highly significant difference between functional and non-functional stapedial groups (Mann–Whitney, $p < 0.001$). This pattern can also be seen in Fig. 5, which shows representative stapedes from taxa with the four main cranial circulation patterns found in extant primates.

Fossil euarchontans and comparison to extant representatives

High resolution X-ray CT models of the stapedes for *Ignacius graybullianus* (USNM 482353) and *Plesiadapis tricuspidens* (MNHN BR 17418) are presented in Fig. 6. For comparison, models of representatives of extant euarchontan orders are also provided, including *Tarsius spectrum*, *Ptilocercus lowii*, and *Galeopterus variegatus*. This figure demonstrates that the fossil ossicles are fully intact and preserve delicate features such as the process for the insertion of the stapedius muscle. Although the higher resolution scans for *I. graybullianus* provide more detail, the similarity of the model for *P. tricuspidens* to a previously described stapes for this

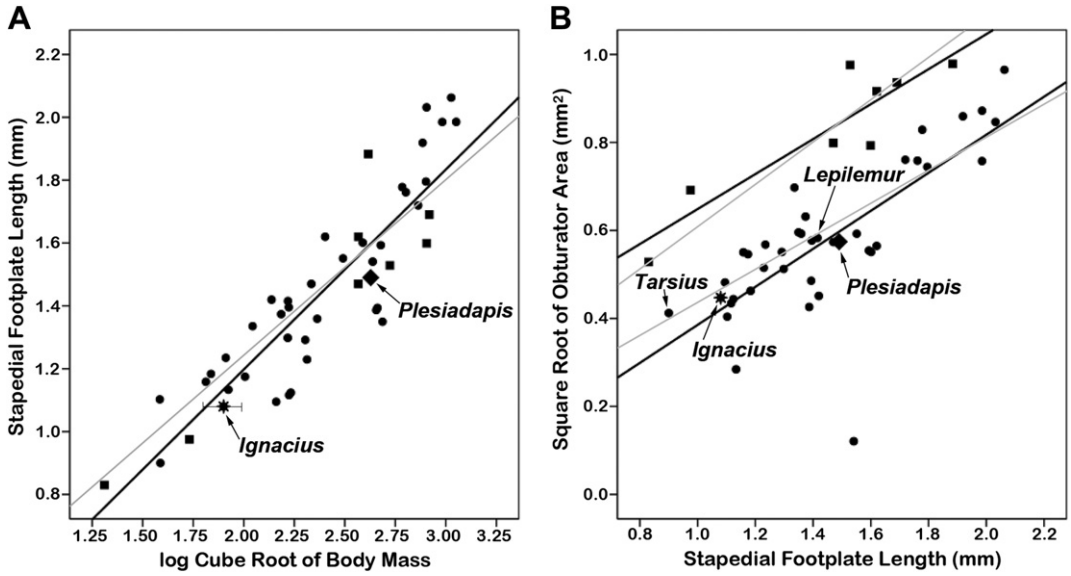

Figure 4. Squares represent taxa with a functional stapedial artery, circles represent taxa with a non-functional stapedial artery, the "star" represents *Ignacius graybullianus* (USNM 482353), and the diamond represents *Plesiadapis tricuspidens* (MNHN BR 17418). Black regression lines defined using conventional statistical techniques. Light grey regression lines based on phylogenetic comparative methods. A. Scatterplot of stapedial footplate length over the log of cube root of body mass. A significant relationship ($p < 0.001$, $r^2 = 0.798$) was found for the entire sample but no difference was detected in relative stapedial footplate length between groups. B. Scatterplot of obturator foramen area over stapedial footplate length. A significant difference was found for relative obturator foramen area between functional and non-functional stapedial groups. The values for USNM 482353 (*I. graybullianus*) and MNHN BR 17418 (*P. tricuspidens*) indicate that these species likely did not have a functional stapedial artery.

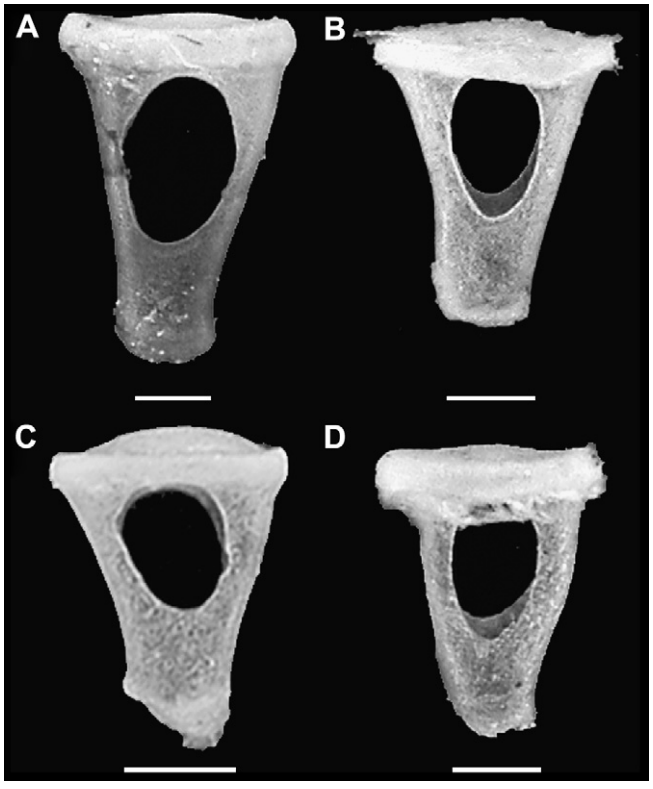

Figure 5. Images of representative stapedes for the four major cranial arterial patterns found in primates (see text for description of patterns associated with each group). A: *Propithecus diadema*; B: *Lepilemur mustelinus*; C: *Loris tardigradus*; D: *Aotus nancymae*. All stapedes scaled to approximately the same size (based on footplate length) with individual scale bars = 0.5 mm. Note the relatively larger foramen for *P. diadema*, which has a functional stapedial artery.

species (Russell, 1964: Fig. 16) adds confidence to the reconstruction presented here.

In general, both fossil specimens share several characteristics in morphology. For example, the footplate is generally concave laterally along the edges, although the center of the footplate bulges somewhat toward what would be the inner ear in anatomical position. A similar morphology is commonly observed in a variety of taxa ranging from squirrels to anteaters (Doran, 1878; Novacek and Wyss, 1986), including numerous species of primates (including all circulation patterns investigated here). However, note that the euarchontans *P. lowii* and *G. variegatus* lack development of the concave region. In addition, the stapedial footplate in both fossil specimens is generally oval in outline, but is slightly more tapered on the posterior edge, giving it a faintly piriform appearance. One unique feature of the *Ignacius* stapes not seen in the *Plesiadapis* stapes, or any other stapedes of any other euarchontans we have examined, relates to the area where the anterior crus approaches the stapedial footplate (Fig. 6). In USNM 482353, the crus divides into three strut-like columns, separated by two fossae. Although the functional consequence of this morphology is unknown, it seems possible to be related to increasing the mechanical strength of the stapes in this area. In addition, note that while *G. variegatus* also has a "strut-like column" of sorts, it is fundamentally different in construction. Instead of flaring outward from the anterior crus, as in *Ignacius*, it flares inward, and, consequently, partially obstructs the obturator foramen. However, this morphology (i.e., internal strut) was not observed in the contralateral stapes for this specimen, or from either of the stapedes from the other species of colugo (*Cynocephalus volans*) examined here.

Based on the relationship between stapedial artery development and the relative size of the obturator foramen in extant euarchontans, the absence or presence of a functional stapedial artery was investigated using the stapedes of *I. graybullianus* (USNM 482353) and *P. tricuspidens* (MNHN BR 17418). Whether the obturator foramina of USNM 482353 and MNHN BR 17418 are relatively large or small is difficult to judge qualitatively (Fig. 6). However, when compared with the extant sample quantitatively, they fall unambiguously with the "non-functional stapedial artery"

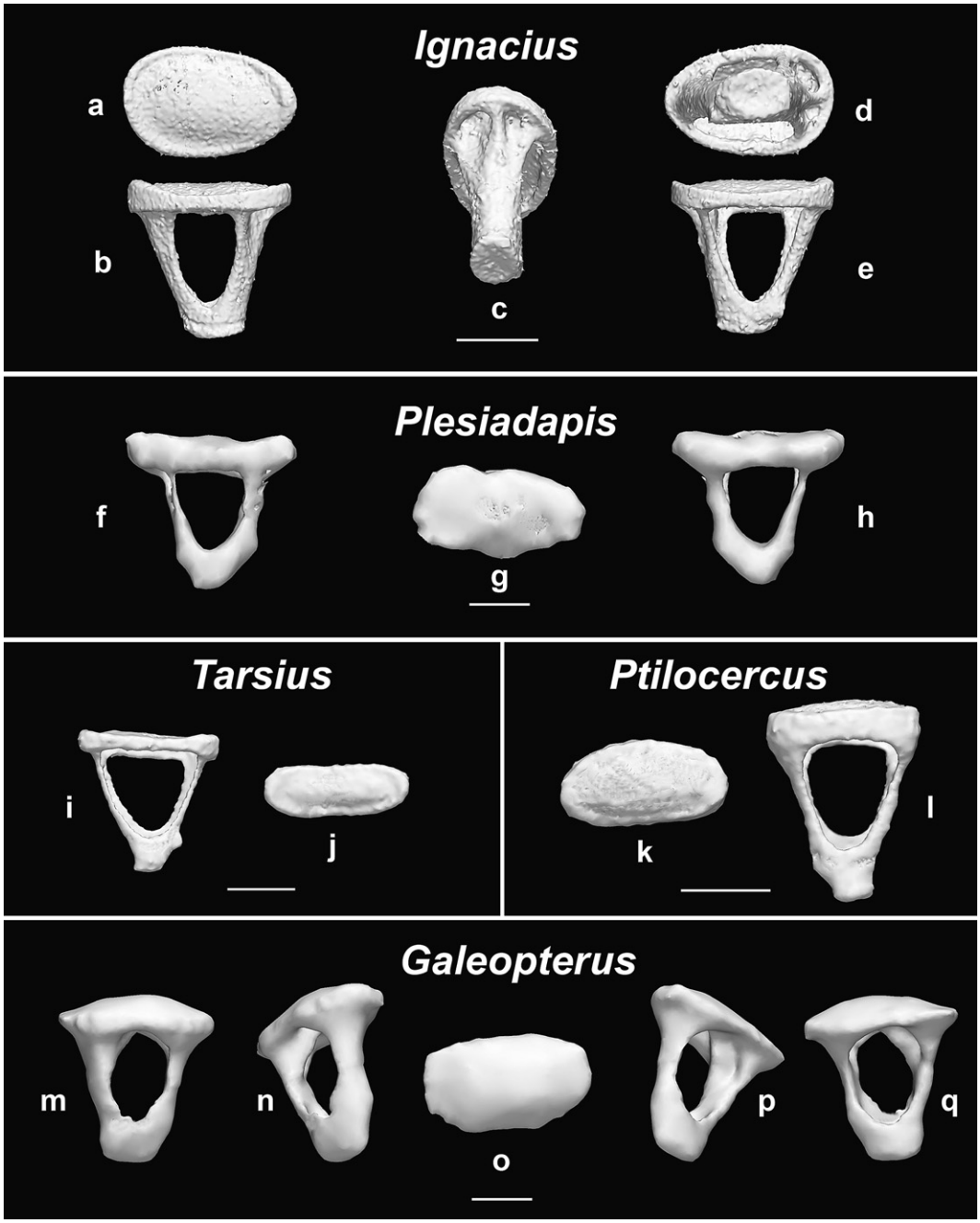

Figure 6. CT models of stapedes for the two fossil taxa (USNM 482353: *Ignacius graybullianus* and MNHN BR 17418: *Plesiadapis tricuspidens*) and three representative extant euarchontans examined in this study (individual scale bars = 0.5 mm). The relative size of the obturator foramen suggests that the fossil specimens did not have a functional stapedial artery. Also, note the unusual morphology of the anterior crus in *I. graybullianus* in which the crus divides into three strut-like processes as they approach the stapedial footplate. Orientations for stapedes as follows: a = medial view; b = dorsal view; c = anterolateral view; d = lateral view; e = ventral view; f = ventral view; g = medial view; h = dorsal view; i = dorsal view; j = medial view; k = medial view; l = ventral view; m = dorsal view; n = oblique posterodorsal view; o = medial view; p = oblique posteroventral view; q = ventral view.

group (Fig. 4B), regardless of which regression technique was used (conventional or phylogenetic). Furthermore, the value of the ratio of the square root of obturator foramen area to stapedial footplate length in USNM 482353 (0.41) and MNHN BR 17418 (0.39) are both within the range of values seen in the non-functional group (0.06–0.52), and outside the range of those representing the functional group (0.50–0.71) (Table 1). In looking at the attachment point of the crura on the footplate (Fig. 6), it becomes obvious as to why the fossils *G. variegatus* and *Tarsius* have a significantly smaller obturator foramen than *P. lowii*: in *P. lowii* and other taxa with a functional stapedial artery, the crura tend to meet the footplate at its lateral margins, whereas in taxa without a stapedial artery, the footplate extends beyond the crura.

Discussion

Two extant taxa have been singled out in Fig. 4B and will be briefly discussed. First, the size of the obturator foramen in *Lepilemur* is of interest, because this species belongs to one of two families of extant lemurs that do not retain a functional stapedial

artery. Instead, the stapedial artery has been reported to be diminutive in this genus (Szalay and Katz, 1973; Schwartz and Tattersall, 1987), and the value for *Lepilemur mustelinus* falls very close to both the conventional and phylogenetic regression lines defined by the non-functional stapedial taxa (Fig. 4B). This pattern is also demonstrated in Fig. 5, where it can be seen that the relative size of the obturator foramen in *Lepilemur* more closely resembles those of *Aotus nancymae* and *Loris tardigradus* (species with a non-functional stapedial a.) than of *Propithecus diadema* (with a functional stapedial a.).

The size of the obturator foramen in tarsiers also deserves mention. Although tarsiers are similar to anthropoids in that they have a relatively large internal carotid artery, they differ in that the stapedial artery may not always completely involute as it does in anthropoids (MacPhee and Cartmill, 1986). In fact, tarsiers maintain a small stapedial canal while no known living anthropoids have been reported to possess a canal for the stapedial artery. While there is debate as to whether or not this canal contains an intact stapedial artery in adult forms (Hill, 1953; Saban, 1963), all of the specimens examined here did show a small, but patent lumen along the entire course of the canal. However, the internal diameter of the canal[1] averaged around 0.1 mm in the specimens we examined, compared to a value of just over 0.3 mm in *Ptilocercus*. This is a substantial difference, considering the fact that tarsiers have a body mass roughly twice that of pen-tailed treeshrews, yet a stapedial canal with a diameter that is three times smaller. This results in the internal area of the stapedial canal being nine times larger in *Ptilocercus* compared to *Tarsius*.

Alternatively, the stapedial canal in adult tarsiers may not contain a patent artery, but is formed during fetal development before the stapedial artery becomes partially or fully obliterated. This is supported by the limited ontogenetic evidence in anthropoids, showing that a stapedial stem is present during development even though a stapedial artery is not retained postnatally (e.g., golden lion tamarins: MacPhee and Cartmill, 1986). Regardless of whether or not the stapedial canal transmits a small artery, the relative size of the obturator foramen in tarsiers appears to be more similar to that of taxa with a non-functional stapedial artery (Fig. 4B). In fact, considering the phylogenetically informed regression analysis in the current study, the value for tarsiers falls almost exactly on the non-functional stapedial taxa line.

Functional implications

A fundamental question raised by our findings is: why do species with a functional stapedial artery appear to have a relatively larger obturator foramen? The answer may have to do with acoustic function. Several researchers have noted that the pulsating walls of arteries in the ear caused by the cardiac (systolic–diastolic) cycle produce pressure waves that can interfere with hearing sensitivity (Fleischer, 1978; Packer, 1983; Diamond, 1989). This is particularly relevant for the stapedial artery because of its close proximity to the stapes as it passes through the obturator foramen. In fact, Diamond (1989: p. 76) has suggested that "it is possible that a minimum clearance…is necessary to allow the pressure wave intensity to attenuate to a degree that would render the waves less likely to interfere with sound transmission through the ossicular chain."

It may be envisioned that natural selection could employ various anatomical strategies to help minimize the problem of physiological noise in the ear. An obvious solution would be to relocate the stapedial artery so that it does not pass through the obturator foramen. However, among all mammals with a stapedial artery, only the monotreme *Ornithorhynchus* (duck-billed platypus) has an artery that does not pass through the stapes (Wible, 1984). Adult monotremes have columellar-shaped stapedes that lack an obturator foramen altogether (Novacek and Wyss, 1986).

Another alternative is to encase the transcrural portion of the stapedial artery in a bony canal (stapedial canal), which has been demonstrated to attenuate arterial sound by 5–15 dB (Packer, 1983). Yet, the sound pressure level of arterial vibrations in the ear can be greater than 100 dB at very low frequencies (Packer, 1983), potentially impacting the motion of the stapes if the crura are too close to the canal walls (Diamond, 1989). Another strategy is simply to reduce or eliminate the stapedial artery altogether and annex its peripheral branches by other vessels – a pattern that is very common among living mammalian groups. Lastly, a few taxa such as the Norway rat (*Rattus norvegicus*) and golden hamster (*Mesocricetus auratus*) have developed a narrowing (coarctation) of the stapedial artery as it passes through the obturator foramen, which apparently reduces disruptive arterial vibrations (Diamond, 1989). The stapedial artery in treeshrews may also show some coarctation as it passes through the obturator foramen based on a narrowing of the stapedial canal in this region (Wible, 2009). One limitation of this mechanism is that volumetric flow rate of blood downstream of the coarctation is diminished (Diamond, 1989), which could be problematic in species that are highly visually dependant (such as anthropoids) because the superior ramus of the stapedial normally supplies most orbital structures.

With these considerations in mind, it seems possible that the relatively larger area of the obturator foramen in species with a functional stapedial artery could be an adaptation that helps reduce acoustic disturbances caused by arterial pulsations. This may also explain why tarsiers have an obturator foramen size that groups more closely with taxa that have a non-functional stapedial artery. Although tarsiers have a stapedial canal, the vestigial vessel that courses through it may not have a continuous patent lumen, and therefore would not be capable of producing arterial pulsations. Even if an intact stapedial artery does occur in tarsiers, vessels with a diameter less than 0.2 mm produce pulsatile sounds with an attenuated amplitude and frequency range (Packer, 1983). These sounds would be further reduced by the presence of a bony canal, and, consequently, there may not be strong selection towards maintaining (or developing) a large obturator foramen.

Phylogenetic implications

In recent years, there has been some debate as to the presence of the internal carotid artery in *Ignacius* (Kay et al., 1992; Bloch and Silcox, 2001; Silcox, 2003). However, virtually all researchers involved agree that if the internal carotid was present, it was likely non-functional. In contrast, there have been shifting opinions about the internal carotid circulation pattern in *Plesiadapis*. Originally, Russell (1959) stated that the distal internal carotid and stapedial arteries were of about equal size in *P. tricuspidens*, based upon grooves left on the promontorium of a nearly complete skull. However, after a report by Saban (1963), which noted the inconsistent patterns of the promontorial grooves in *P. tricuspidens*, Russell altered his interpretation to conclude that if a stapedial branch was present, it was reduced (Russell, 1964). This interpretation was later affirmed by Gingerich (1976) when he stated that, in general, the internal carotid system was greatly reduced in Plesiadapidae, and that the stapedial branch was apparently vestigial. Hence, it is now generally agreed that both *Ignacius* and *Plesiadapis* had a greatly reduced internal carotid system and that neither shows evidence for a functional stapedial artery. This conclusion is supported by the

[1] Canals were measured on CT models at the proximal end of the transcrural portion of the stapedial canal. All methods and specimens used are the same as those used to create CT models of the stapedes described above.

finding that obturator foramen size in both *I. graybullianus* and *P. tricuspidens* is proportionally similar to taxa lacking a functional stapedial artery.

The lack of a functional internal carotid artery, stapedial artery, and small stapedial obturator foramen are characters that these plesiadapiforms share with dermopterans to the exclusion of scandentians or primitive modern primates. What such similarities mean in terms of the evolutionary history of these taxa depends on the pattern of inter-relationships among euarchontans.

Views of inter-relationships among different extant and fossil euarchontans have been historically contentious for morphologists. Kay et al. (1992) presented the first phylogenetic hypothesis based on a cladistic analysis for the placement of plesiadapiforms (*Ignacius* and *Plesiadapis*) among primates, dermopterans, scandentians, chiropterans, and erinaceomorphs using cranial data (33 characters). They recovered plesiadapiforms as the sister taxon to dermopterans. This group was basal to a clade in which a Primates-Scandentia group was the sister to Chiroptera with erinaceomorphs basal to this. Beard (1993) presented another phylogenetic hypothesis for plesiadapiforms (based on cladistic analysis of 28 postcranial characters and 1 cranial character), and also recovered *Ignacius* as the sister taxon of dermopterans (Eudermoptera), while other plesiadapiforms were stem-members of Eudermoptera. This dermopteran clade (including plesiadapiforms) formed the sister taxon to modern Primates. He called this grouping Primatomorpha. Primatomorpha was, in turn, the sister group to chiropterans in his analysis, and Scandentia was the sister group to this even larger clade. Bloch et al. (2007) presented an alternative view resulting from cladistic analysis of a character matrix with much greater sampling of morphological characters and taxa, including plesiadapiforms, other fossil euarchontans, outgroups, and extant euarchontans. Theirs was the first peer-reviewed analysis to extensively sample crania, postcrania, and dental remains in a single matrix for addressing this question (173 characters total). They found dermopterans and scandentians to form a sister taxon, while plesiadapiforms were found to be related to modern Primates as successive stem members, more consistent with pre-parsimony views (e.g., Simpson, 1935; Szalay et al., 1987). Molecular data originally supported the hypothesis that Scandentia and Dermoptera are a clade (Murphy et al., 2001). More recent analyses using data from short interspersed nuclear elements (SINEs) and more species of scandentians (Janečka et al., 2007) now suggest that dermopterans and primates form a clade to the exclusion of treeshrews. Furthermore, in some molecular analyses, scandentians are placed among Glires (e.g., Waddell and Shelley, 2003). Parsimony analysis of the Bloch et al. (2007) matrix using a topological constraint matching the tree from Janečka et al. (2007), still places plesiadapiforms as stem primates (Janečka et al., 2007). Yet, given conflicting results of other recent analyses, it is only fair to say that relationships among extant euarchontans are unresolved. Specifically, Nie et al. (2008) still recovered evidence for a treeshrew + dermopteran clade (Sundatheria) using chromosomal painting, while Liu et al. (2009) recovered a treeshrew + primate clade using molecular coalescence.

Under Beard's hypothesis (1990, 1993), the dermopteran–plesiadapiform similarities in obturator foramen size are synapomorphies. Under Bloch et al. (2007), the pattern of evolution is ambiguous: they are either convergently acquired or primitive for Euarchonta, because the sister taxon of Plesiadapidae (Carpolestidae) will most likely not exhibit them, as it probably had a functional stapedial artery (Bloch and Silcox, 2006). Under a modified version of Bloch et al. (2007), in which dermopterans are the sister taxon of modern primates + plesiadapiforms, these similarities are either convergent or synapomorphies of Dermoptera + Primates that were "reversed" in basal modern primates and carpolestids.

Previous studies have suggested that the size and functionality of cranial arteries are labile at an ordinal level (Wible and Martin, 1993). This is supported by the observation of diversity in stapedial development even within Lemuridae. Features such as the route traversed by the internal carotid system (=internal carotid artery and/or nerve plexus) across the promontorium have been proposed to be less labile (Wible, 1993). In this case, modern primates and plesiadapiforms are similar in exhibiting evidence that the internal carotid system was shifted unusually far to the lateral side of the promontorium (e.g., Bloch and Silcox, 2001; Bloch et al., 2007). Dermopterans and scandentians exhibit the more commonly seen state in which the internal carotid system is more medially positioned (note that in dermopterans the internal carotid system consists of only the nerve plexus as the arterial component involutes during ontogeny; Wible, 1993). Our study of the stapes and stapedial artery provides another example for which anatomical routes of cranial neurovasculature (and osteological correlates thereof) exhibit low variability compared to the size (and functionality) of the arteries that use these routes: *Tarsius* retains the bony tube for the stapedial artery, though the artery is apparently non-functional. The fact that many eutherians retain a bicrurate stapes, even though the stapedial artery is absent in the adult, also provides evidence of the conserved position of the stapedial artery in early ontogeny, based on our results that suggest that the obturator foramen functions to allow passage of a stapedial artery. The hypothesis that the obturator foramen reflects the fetal position of the stapedial artery in taxa that lack this vessel as adults, is further supported by the observation that the obturator foramen is known to be absent in the one living mammal whose patent stapedial artery does not pass through the stapes (*Ornithorhynchus*; Wible, 1984). On the other hand, the existence of a bicrurate stapes and an extra-ossicular stapedial artery (the combined presence of which would refute our hypothesis) is undocumented.

Because this study confirms that cranial arterial functionality is labile compared to arterial position, the confirmation that some plesiadapiforms are like dermopterans in the lack of a functional stapedial artery, does not greatly affect previous perspectives on euarchontan higher level relationships by itself; however, it does add weight to the observation that plesiadapiforms and primates are similar in having the internal carotid system cross the promontorium laterally. Furthermore, this study adds to a growing body of new character information that should ultimately provide more confident perspectives on various phylogenetic issues.

Summary and conclusions

Our data suggest that the relative size of the obturator foramen in euarchontans is determined by the presence or absence of a functional stapedial artery. Therefore, in combination with evidence from other taxa exhibiting different arterial patterns, we interpret these results to show that the obturator foramen exists in order to transmit the stapedial artery at some point in ontogeny. We anticipate that this new line of evidence for evaluating the presence of a functional stapedial artery will provide new information related to the polarity and dominance of cranial circulation patterns in other primate fossil taxa, and contribute to future discussions of primate evolutionary relationships. Future studies should extend this analysis to non-euarchontan eutherians and the bewildering array of arterial patterns they display.

Acknowledgments

The authors would like to thank Marc Godinot, Alan Walker, and Jon Bloch for permission to examine the fossil specimens. We thank Tim Ryan, Alan Walker, and Erik Seiffert for access to and

permission to use high resolution x-ray computed tomography scans of *Cynocephalus volans* and *Galeopterus variegatus*. We thank Jack T. Stern, Jr., Nate Kley, and Randy Nydam for providing access to imaging equipment, and Ian Wallace for translating sections of Russell (1964). We also thank the editors (Steve Leigh, Jon Bloch), Mary Silcox, John Wible, and one anonymous reviewer for helpful comments on the manuscript. M.N.C. received funding for other high resolution x-ray computed tomography scans and museum travel from the National Science Foundation (NSF BCS-0408035), Midwestern University, and Stony Brook University. Grants to D.M.B. include those from the National Science Foundation (NSF BCS-0622544), the Evolving Earth Foundation, and the American Society of Mammalogists.

References

Archibald, J.D., 1977. Ectotympanic bone and internal carotid circulation of eutherians in references to anthropoid origins. J. Hum. Evol. 6, 609–622.

Askay, S., 2000. "*Ptilocercus lowii*" (On-line), Animal Diversity Web. http://animaldiversity.ummz.umich.edu/site/accounts/information/Ptilocercus_lowii.html (accessed 05.03.10).

Beard, K.C., 1990. Gliding behavior and paleoecology of the alleged primate family Paromomyidae (Mammalia, Dermoptera). Nature 345, 340–341.

Beard, K.C., 1993. Phylogenetic systematics of the Primatomorpha, with special reference to Dermoptera. In: Szalay, F.S., McKenna, M.C., Novacek, M.J. (Eds.), Mammal Phylogeny: Placentals. Springer-Verlag, New York, pp. 129–150.

Bininda-Emonds, O., Cardillo, M., Jones, K., MacPhee, R., Beck, R., Grenyer, R., Price, S., Vos, R., Gittleman, J., Purvis, A., 2007. The delayed rise of present-day mammals. Nature 446, 507–512.

Bloch, J.I., Silcox, M.T., 2001. New basicrania of Paleocene–Eocene *Ignacius*: re-evaluation of the plesiadapiform–dermopteran link. Am. J. Phys. Anthropol. 116, 184–198.

Bloch, J.I., Silcox, M.T., 2006. Cranial anatomy of the Paleocene plesiadapiform *Carpolestes simpsoni* (Mammalia, Primates) using ultra high-resolution X-ray computed tomography, and the relationships of plesiadapiforms to euprimates. J. Hum. Evol. 50, 1–35.

Bloch, J.I., Silcox, M.T., Boyer, D.M., Sargis, E.J., 2007. New Paleocene skeletons and the relationship of plesiadapiforms to crown-clade primates. Proc. Natl. Acad. Sci. USA 104, 1159–1164.

Bugge, J., 1974. The cephalic arterial system in insectivores, primates, rodents and lagomorphs with special reference to systematic classification. Acta Anat. 87, 1–160.

Butler, H., 1980. The homologies of the lorisoid internal carotid artery system. Int. J. Primatol. 1, 333–343.

Cartmill, M., 1975. Strepsirhine basicranial structures and the affinities of the Cheirogaleidae. In: Luckett, W.P., Szalay, F.S. (Eds.), Phylogeny of the Primates: A Multidisciplinary Approach. Plenum Press, New York, pp. 313–354.

Cartmill, M., MacPhee, R.D.E., 1980. Tupaiid affinities: the evidence of the carotid arteries and cranial skeleton. In: Luckett, W.P. (Ed.), Comparative Biology and Evolutionary Relationships of Tree Shrews. Plenum Press, New York, pp. 95–132.

Coleman, M.N., Colbert, M., 2007. Technical note – a brief report on thresholding protocols for taking measurements on three-dimensional digitally generated models. Am. J. Phys. Anthropol. 133, 723–725.

Coleman, M.N., Ross, C.F., 2004. Primate auditory diversity and its influence on hearing performance. Anat. Rec. 281A, 1123–1137.

Conroy, G.C., Wible, J.R., 1978. Middle ear morphology of *Lemur variagatus*. Folia Primatol. 29, 81–85.

Cortés-Ortiz, L., Bermingham, E., Rico, C., Rodríguez-Luna, E., Sampaio, I., Ruiz-García, M., 2003. Molecular systematic and biogeography of the neotropical monkey genus, *Alouatta*. Mol. Phylogenet. Evol. 26, 64–81.

Diamond, M.K., 1989. Coarctation of the stapedial artery: an unusual adaptive response to competing functional demands in the middle ear in some eutherians. J. Morphol. 200, 71–86.

Diamond, M.K., 1991. Homologies of the stapedial artery in humans, with a reconstruction of the primitive stapedial artery configuration in euprimates. Am. J. Phys. Anthropol. S4, 433–462.

Doran, A.H.G., 1878. Morphology of the mammalian ossicula auditus. Trans. Linn. Soc. Ser. 2, Zool. 1, 371–497.

Fleischer, G., 1978. Evolutionary principles of the mammalian middle ear. Advan. Anat. Embry. Cell Biol. 55, 1–70.

Gingerich, P.D., 1973. Anatomy of the temporal bone in the Oligocene anthropoid *Apidium* and the origin of Anthropoidea. Folia Primatol. 19, 329–337.

Gingerich, P.D., 1976. Cranial Anatomy and Evolution of the Early Tertiary Plesiadapidae (Mammalia, Primates), vol. 5. Univ. Mich. Pap. Paleontol., pp. 1–141.

Hafferl, A., 1916. Zur entwicklungsgeschichte der aortenbögen und kopfarterien von *Tarsius spectrum*. Gegen. Morphol. Jb. 50, 19–48.

Hill, W.C.O., 1953. Primates: Comparative Anatomy and Taxonomy, vol. 1. Strepsirhini. Edinburgh University Press, Edinburgh.

Hodgson, J., Sterner, K., Matthews, L., Burrell, A., Jani, R., Raaum, R., Stewart, C., Disotell, T., 2009. Successive radiations, not stasis, in the South American primate fauna. Proc. Natl. Acad. Sci. USA 106, 5534–5539.

Horvath, J., Weisrock, D., Embry, S., Fiorentino, I., Balhoff, J., Kappeler, P., Wray, G., Willard, H., Yoder, A., 2008. Development and application of a phylogenomic toolkit: resolving the evolutionary history of Madagascar's lemurs. Genom. Res. 18, 489.

Janečka, J.E., Miller, W., Pringle, T.H., Wiens, F., Zitzmann, A., Helgen, K.M., Springer, M.S., Murphy, W.J., 2007. Molecular and genomic data identify the closest living relative of primates. Science 318, 792–794.

Kanagasuntheram, R., Krishnamurti, A., 1965. Observations on the carotid rete in the lesser bush baby (*Galago senegalensis*). J. Anat. 99, 861–875.

Kay, R.F., Ross, C., Williams, B.A., 1997. Anthropoid origins. Science 275, 797–804.

Kay, R.F., Thewissen, J.G.M., Yoder, A.D., 1992. Cranial anatomy of *Ignacius graybullianus* and the affinities of the Plesiadapiformes. Am. J. Phys. Anthropol. 89, 477–498.

Liu, L., Yu, L., Pearl, D.K., Edwards, S.V., 2009. Estimating species phylogenies using coalescence time among sequences. System. Biol. 58, 468–477.

MacPhee, R.D.E., 1981. Auditory Regions of Primates and Eutherian Insectivores. Contributions to Primatology, vol. 18. S. Karger, Basel.

MacPhee, R.D.E., 1987. Basicranial morphology and ontogeny of the extinct giant lemur *Megaladapis*. Am. J. Phys. Anthropol. 74, 333–355.

MacPhee, R.D.E., Cartmill, M., 1986. Basicranial structures and primate systematics. In: Comparative Primate Biology, vol. 1. Alan R. Liss, Inc., New York, pp. 219–275. Systematics, Evolution, and Anatomy.

Maddison, W.P., Maddison, D.R., 2010. Mesquite: A Modular System for Evolutionary Analysis. http://mesquiteproject.org Version 2.73.

Menezes, A.N., Bonvicino, C.R., Seuánez, H.N., 2010. Identification, classification and evolution of owl monkeys (*Aotus*, Illiger 1811). BMC Evol. Biol. 10, 1–15.

Midford, P.E., Garland Jr., T., Maddison, W.P., 2010. PDAP Package of Mesquite. http://mesquiteproject.org/pdap_mesquite/ Version 1.15.

Murphy, W.J., Eizirik, E., O'Brien, S.J., Madsen, O., Scally, M., Douady, C.J., Teeling, E., Ryder, O.A., Stanhope, M.J., de Jong, W.W., Springer, M.S., 2001. Resolution of the early placental mammal radiation using Bayesian phylogenetics. Science 294, 2348–2351.

Myers, P., 2000. "Dermoptera" (On-line), Animal Diversity Web. http://animaldiversity.ummz.umich.edu/site/accounts/information/Dermoptera.html (accessed 02.03.10).

Nie, W., Fu, B., O'Brien, P.C.M., Wang, J., Su, W., Tanomtong, A., Volobouev, V., Ferguson-Smith, M.A., Yang, F., 2008. Flying lemurs – the "flying tree shrews"? Molecular cytogenetic evidence for a Scandentia–Dermoptera sister clade. BMC Biol. 6, 18.

Novacek, M.J., Wyss, A., 1986. Origin and Transformation of the Mammalian Stapes. Contib. Geol., Univ. Wyom, Spec. Pap. 3, pp. 35–53.

Opazo, J.C., Wildman, D.E., Prychitko, T., Johnson, R.M., Goodman, M., 2006. Phylogenetic relationships and divergence times among New World monkeys (Platyrrhini, Primates). Mol. Phylogenet. Evol. 40, 274–280.

Packer, D.J., 1983. Physiological noise, carotid arteries, and auditory sensitivity in mammals. New York University, Ph.D. Dissertation.

Russell, D.E., 1959. Le crane de *Plesiadapis*. Note preliminaire. Bull. Soc. Geol. 1, 312–314. France, 7th Series.

Russell, D.E., 1964. Les mammiferes paleocenes d'Europe. Mem. Mus. Nation. Host. Nat. 13, 1–321.

Saban, R., 1963. Contribution à l'étude de l'os temporal des primates. Description chez l'homme et les prosimiens. Anatomie comparée et phylogénie. Mem. Mus. Nation. Host. Nat. 29, 1–378.

Saban, R., 1975. Structure of the ear region in living and subfossil lemurs. In: Tattersall, I., Sussman, R.W. (Eds.), Lemur Biology. Plenum Press, New York, pp. 83–109.

Schwartz, J.H., Tattersall, I., 1987. Tarsiers, adapids and the integrity of Strepsirhini. J. Hum. Evol. 16, 23–40.

Silcox, M.T., 2003. New discoveries on the middle ear anatomy of *Ignacius graybullianus* (Paromomyidae, Primates) from ultra high resolution X-ray computed tomography. J. Hum. Evol. 44, 73–86.

Silcox, M.T., Bloch, J.I., Boyer, D.M., Godinot, M., Ryan, T.M., Spoor, F., Walker, A., 2009b. Semicircular canal system in early primates. J. Hum. Evol. 56, 315–327.

Silcox, M.T., Dalmyn, C.K., Bloch, J.I., 2009a. Virtual endocasts of *Ignacius graybullianus* (Paromomyidae, Primates) and brain evolution in early primates. Proc. Natl. Acad. Sci. USA 106, 10987–10992.

Simpson, G.G., 1935. The Tiffany fauna, upper Paleocene. II – structure and relationships of *Plesiadapis*. Am. Mus. Novit., 1–30.

Smith, R.J., Jungers, W.L., 1997. Body mass in comparative primatology. J. Hum. Evol. 32, 523–559.

Spencer, M.A., Spencer, G.S., 1995. Technical note: video-based three-dimensional morphometrics. Am. J. Phys. Anthropol. 96, 443–453.

Szalay, F.S., 1975. Phylogeny of primate higher taxa: the basicranial evidence. In: Luckett, W.P., Szalay, F.S. (Eds.), Phylogeny of the Primates. Plenum Press, New York, pp. 91–125.

Szalay, F.S., Katz, C., 1973. Phylogeny of lemurs, galagos and lorises. Folia Primatol. 19, 88–103.

Szalay, F.S., Rosenberger, A.L., Dagosto, M., 1987. Diagnosis and differentiation of the order Primates. Yearb. Phys. Anthropol. 30, 75–105.

Tavaré, S., Marshall, C.R., Will, O., Soligo, C., Martin, R.D., 2002. Using the fossil record to estimate the age of the last common ancestor of extant primates. Nature 416, 726–729.

Tosi, A.J., Detwiler, K.M., Disotell, T.R., 2005. X-chromosomal window in to the evolutionary history of the guenons (Primates: Cercopithecini). Mol. Phylogenet. Evol. 36, 58–66.
Waddell, P.J., Shelley, S., 2003. Evaluating placental inter-ordinal phylogenies with novel sequences including RAG1, g-fibrinogen, ND6, and mt-tRNA, plus MCMC-driven nucleotide, amino acid, and codon models. Mol. Phylogenet. Evol. 28, 197–224.
Wahlert, J.H., 1974. The cranial foramina of protrogomorphous rodents: an anatomical and phylogenetic study. Bull. Mus. Comp. Zool. 146, 363–410.
Wible, J.R., 1983. The internal carotid artery in early eutherians. Paleontol. Pol. 28, 281–293.
Wible, J.R., 1984. The ontogeny and phylogeny of the mammalian cranial arterial pattern. Duke University, Ph.D. Dissertation.
Wible, J.R., 1986. Transformations in the extracranial course of the internal carotid artery in mammalian phylogeny. J. Vert. Paleontol. 6, 313–325.
Wible, J.R., 1987. The eutherian stapedial artery: character analysis and implications for superordinal relationships. Zool. J. Linn. Soc. 91, 107–135.
Wible, J.R., 1993. Cranial circulation and relationships of the colugo *Cynocephalus* (Dermoptera, Mammalia). Am. Mus. Novit. 3072, 1–27.
Wible, J.R., 2009. The ear region of the pen-tailed treeshrew, *Ptilocercus lowii* Gray, 1848 (Placentalia, Scandentia, Ptilocercidae). J. Mamm. Evol. 16, 199–233.
Wible, J.R., Martin, J.R., 1993. Ontogeny of the tympanic roof in archontans. In: MacPhee, R.D.E. (Ed.), Primates and Their Relatives in Phylogenetic Perspective. Plenum Press, New York, pp. 111–148.
Wible, J.R., Davis, D.L., 2000. Ontogeny of the chiropteran basicranium, with reference to the Indian false vampire bat, Megaderma lyra. In: Adams, R.A., Pedersen, S.C. (Eds.), Ontogeny, Functional Ecology, and Evolution of Bats. Cambridge University Press, Cambridge, pp. 214–246.
Wible, J.R., Zeller, U., 1994. Cranial circulation of the pen-tailed tree shrew *Ptilocercus lowii* and relationships of scandentia. J. Mamm. Evol. 2, 209–230.
Yoder, A., Yang, Z., 2004. Divergence dates for Malagasy lemurs estimated from multiple gene loci: geological and evolutionary context. Mol. Ecol. 13, 757–773.